Molecularly Imprinted Chitosan−Genipin Hydrogels with Recognition Capacity toward *o*-Xylene

Bibiana M. Espinosa-García,[†] Waldo M. Argüelles-Monal,[‡] Javier Hernández,[†] Leticia Félix-Valenzuela,[†] Niuris Acosta,[§] and Francisco M. Goycoolea*,[†]

Laboratory of Biopolymers, Centro de Investigación en Alimentación y Desarrollo (CIAD), P.O. Box 1735, Hermosillo, Sonora 83000 Mexico, CIAD-Unidad Guaymas, Carretera al Varadero Nacional Km 6.6, Guaymas, Sonora 85400, Mexico, and Instituto de Estudios Biofuncionales, Universidad Complutense de Madrid, Paseo Juan XXIII No. 1, Madrid 28040, Spain

Received April 25, 2007; Revised Manuscript Received July 30, 2007

A molecularly imprinted material was developed from hydrogels of chitosan (CS) cross-linked with genipin (GNP) using *o*-xylene as the template molecule. Gelling time, mechanical, and diffusion properties of CS−GNP hydrogels were initially investigated to establish optimal conditions to prepare molecularly imprinted hydrogels (MIHs). The elastic modulus was found to be directly proportional to the degree of cross-linking (R = moles of genipin/moles of glucosamine) while the diffusion of water, as monitored by magnetic resonance imaging, decreased with R. CS−GNP hydrogels of varying R were imprinted with *o*-xylene ($MIH_{o\text{-xylene}}$). The adsorption capacity of *o*-xylene by $MIH_{o\text{-xylene}}$ was greater than the corresponding control hydrogels, particularly at $R = 0.25$. Freundlich isotherms yielded a better fitness than Langmuir ones and afforded n and Q_{max}values of 2.55 and 103.3 mg/g, respectively. The imprinted hydrogel showed the highest adsorption capacity for *o*-xylene; however, the material was not highly selective as it also exhibited the capacity to adsorb *m*- and *p*-xylene isomers. In turn, the $MIH_{o\text{-xylene}}$ showed a low adsorption when 2-fluorotoluene was used in rebinding experiments, suggesting that molecular recognition by the binding sites is influenced by the electronic and steric properties of the analyte molecule, thus effectively confirming the imprinting effect within the $MIH_{o\text{-xylene}}$ network. This work opens the possibility to future development of materials with the capacity to adsorb *o*-xylene analogue molecules such as contaminants bearing chlorinated aromatic structures.

Introduction

Molecular imprinting is a recently developed technique aimed to prepare polymeric materials with specific recognition toward a specific molecule.[1−3] Molecularly imprinted polymer materials (MIPs) have been considered as artificial receptors, and their main application area so far has been in analytical chemistry (separation processes, sensors, artificial antibodies, and controlled drug delivery).[4] In its original conception, molecular imprinting of polymers involves the formation of a prepolymerization complex between a functional monomer and a template molecule through either covalent[5,6] or noncovalent[7,8] interactions or by metal ion coordination.[9−11] The complex is then polymerized using a cross-linking agent, and later the template is extracted from the polymer to free the created molecular recognition sites. The resulting MIP has steric and chemical memory toward the template and hence could be used to rebind it.[12,13] When the template molecule is toxic, unstable, or expensive, the use of analogue compounds with a chemical structure that shares features of the template molecule seems to be a good alternative.[14−20]

More recently, the molecular imprinting concept also has been applied to the development of materials in the gel state. Thes types of materials are formed with lower cross-linking densities than traditional MIPs; hence they are more flexible and possess a greater conformational freedom.[21,22] Gels' inherent characteristics allow the prepararion of films, monoliths, beads, and nanoparticles that can be used in the development of advanced materials for sensors, antibody replacements, chromatography columns, and microextraction devices due to their better adhesion to sensor surfaces than traditional MIPs.[23,24] At the cutting edge of research in MIP gel systems are those that present analyte specificity and responsiveness to external stimuli.[21]

The use of natural polymers for preparing molecularly imprinted materials has prompted interest, particularly due to their potential application in drug delivery.[13] Chitosan is a polysaccharide with a firmly established capacity to form hydrogels under varying chemical or physical conditions to meet different purposes in a wide range of applications.[25−29]

Molecular imprinting of chitosan hydrogels has only just started to be explored. In this regards, the well-advocated advantages of chitosan, namely, its abundance, nontoxicity, biodegradability, and biocompatibility properties,[30] altogether make it an interesting biopolymer for the development of advanced materials. Recently, a new natural cross-linking agent obtained from fruits of *Gardenia jasminoides* Ellis and *Genipa americana*, genipin, has been documented[31] and successfully used in the engineering of chitosan hydrogels for various purposes.[32,33] Genipin is used in traditional Chinese medicine and has been reported to be much less toxic and more biocompatible than glutaraldehyde.[34,35] The use of natural cross-linkers to prepare hydrogels has become a promising alternative to prepare fully biocompatible materials.[36−38]

* Author to whom correspondence should be addressed. Phone: +52-662-289-2400 (ext. 248). Fax: +52-662-280-0055. E-mail: fgoyco@cascabel.ciad.mx.

[†] Centro de Investigación en Alimentación y Desarrollo.

[‡] CIAD-Unidad Guaymas.

[§] Universidad Complutense de Madrid.

10.1021/bm700458a CCC: $37.00
Published on Web 10/18/2007

As far as we are aware, only few very recent works, published by two independent groups, have addressed chitosan-based molecularly imprinted hydrogels, namely, those by Aburto et al. at the Mexican Petroleum Institute, who developed a chitosan/gluteraldehyde hydrogel to selectively adsorb dibenzothiophene sulfone (DBTS), an organosulfur compound that contributes to catalyst poisoning and equipment corrosion during petroleum refining,[39,40] and those by Guo et al. and Xia et al. at the Institute of Polymer Chemistry, Nankai University, China, who had developed molecularly imprinted hydrogel matrixes based on a chitosan and acrylamide semi-interpenetrating polymer network to recognize hemoglobin.[41,42]

In this work, we have selected *o*-xylene as a model template due to its structural similarity to polychlorinated biphenyl (PCB) congeners, well-known persistent organic pollutants. A similar approach was adopted by Hosoya et al.[18,19] using *o*-, *m*-, and *p*-xylene as porogenic templates to fabricate molecularly imprinted synthetic stationary phases for chromatography based on polystyrene cross-linked with ethylene dimethacrylate (EDMA) monomers. Therefore, the aim of this work was to prepare and evaluate the adsorption capacity and selectivity of a molecularly imprinted hydrogel (MIH) with chitosan acting as the already available constituent polymer, genipin as a natural cross-linking agent, and *o*-xylene as the template.

Experimental Section

Materials. Chitosan (CS) was a purified batch obtained from chitin isolated from shrimp (*Lithopenaeus stilyrostris*) headwaste in the pilot plant facility of the Laboratoty of Biopolymers of the Centro de Investigación en Alimentación y Desarrollo. The degree of acetylation was 10% as determined by ^{1}H NMR in DCl/D_2O on a Bruker AVANCE 400 MHz instrument at 70 °C. To this end, 10 mg of sample was introduced into a 5 mm in diameter NMR test tube to which 0.5 mL of 2% DCl/D_2O (w/w) solution was added, and the tube was kept at 70 °C to fully dissolve the polymer. The viscosimetric molecular mass (M_v) was estimated to be $\sim 7.8 \times 10^4$ Da as determined by viscosimetry in 0.3 M acetic acid/0.2 M sodium acetate at 25 °C, using the Mark−Houwink−Sakurada constants K_η and α, 0.074 and 0.76, respectively ($[\eta] = 385.75$ mL/g).[43] Genipin (GNP) was purchased from Challenge Bioproducts, Ltd (Taiwan). Acetic acid, methanol, ethanol, and sodium hydroxide (99%) were supplied by Merck-Mexico S.A. (Mexico City, Mexico); silicone oil, *o*-, *p*-, and *m*-xylene (≥98%), ninhiydrin (≥98%), ethylene glycol monomethyl ether (≥99.5%), and citric acid were supplied by Fluka Sigma-Aldrich Chemie Gmbh (Steinheim, Germany); $SnCl_2 \cdot 2H_2O$ (98%) was from Panreac Química S.A. (Barcelona, Spain); DCl, D_2O, and 2-fluorotoluene (≥99%) were from Aldrich Chemical Co., Inc. (Milwaukee, WI). All reagents were of analytical grade. Distilled water was used throughout.

Gelation Critical Time (t_{gel}) of CS−GNP Hydrogels. A CS solution at 1.5% (w/w) dissolved in 0.1 M acetic acid at room temperature under magnetic stirring for 12 h was prepared. Genipin (100 mg/mL) was dissolved in methanol. A series of CS−GNP solutions were prepared to investigate the role of molar stoichiometry on gel physical and chemical features. GNP was added to the chitosan solution at $R = 0.05$, 0.1, 0.25, 0.5, and 1.0, where R = moles of genipin/moles of glucosmine, the solutions were vigorously stirred, and a 1.7 mL aliquot of each mixture was used in the rheological experiments.

Rheological Determinations. The rheological properties of the CS−GNP system were investigated using a strain-controlled rheometer (Rheometrics model RFSII fluids spectrometer, Piscattaway, NJ), fitted with a truncated cone-plate (cone angle, 0.0397 rad; diameter, 50 mm; gap, 53 μm) and a circulating environmental system for temperature control. To prevent drying of the samples during experiments with long duration times, a ~60 mm glass ring was placed around the measuring geometry, and the annulus was filled with silicone oil of low viscosity. The evolution of the mechanical properties during the course of the gel formation process was monitored by measurements of storage, $G'(t)$, and loss, $G''(t)$, moduli registered at 40 °C, $\omega = 1.0$ rad/s, and strain values of $\gamma = 0.10$ (within the linear viscoelastic region) of the solutions. The criterion to establish the rheological critical gel time, t_{gel}, was considered as the time elapsed for the tan δ value to be equal to 1.0 (tan $\delta = G''/G'$). At the end of the gelation experiments, mechanical spectra were registered ($\omega = 0.1-100$ rad s^{-1}, $\gamma = 10\%$). The final value of G' at 1 rad/s was considered as G'_{eq}.

Determination of the Extent of Cross-Linking. The extent of cross-linking of chitosan by genipin was determined chemically by the ninhydrin assay according with the protocol described elsewhere[33] using a standard curve of D-glucosamine. The assay determines the percentage of free amino groups remaining in the lyophilized chitosan hydrogels after cross-linking. The determination was made in triplicate.

Determination of the Apparent Diffusion Coefficient by Magnetic Resonance Imaging. Magnetic resonance imaging (MRI) experiments were performed on a BIOSPEC BMT 47/40 (Bruker, Ettlingen, Germany) imaging spectrometer operating at 4.7 T. Magnetic field gradients for imaging in the three orthogonal directions were generated by a 12 cm actively shielded gradient set. Individual hydrogel samples were formed directly in NMR tubes (i.d. = 3 mm, height ≈ 30 mm) truncated from the top. A total of six tubes (five with samples and one with water) were placed in a home-built solenoidal coil (i.d. = 15 mm), and the probe head was placed at the center of the magnet. For the apparent diffusion coefficient (D) measurements a spin−echo diffusion-weighted sequence, with the diffusion gradients applied along the read and phase directions, was used. Separate images were acquired at five diffusion weightings by incrementing the diffusion gradient strength with b values between 100 and 8500 s/mm^2. The acquisition parameters of the images were: time between gradients (Δ) = 50 ms, time of pulse gradient (δ) = 10 ms, repetition time = 2000 ms, echo time = 75 ms, number of accumulations = 2, field of view = 2.56 cm, and slice thickness = 1.0 mm. The D mean values and standard deviation for 10 regions of interest (ROIs) on each gel were calculated using the Image Sequence Analysis utility of the ParaVision 3.0.1 program (Bruker, Ettlingen, Germany). From these parametric maps, we obtained the D mean values and the standard deviation over all of the ROIs that represent all of the area of the gel in the image. D was calculated from a series of diffusion-weighted images at different diffusion gradient strength.

Preparation of CS−GNP−*o*-Xylene Molecularly Imprinted Hydrogels (MIH$_{o\text{-Xylene}}$). To a 1.5% (w/w) CS solution in 0.1 M acetic acid was added an aliquot of *o*-xylene in a 1:10 (moles of *o*-xylene/moles of glucosamine), and the mixture was homogenized at 10 000 rpm for 30 s. Genipin, previously dissolved in methanol at a concentration of 100 mg/mL, was added to the emulsified mixture such that the cross-linking degree, R = moles of genipin/moles of glucosamine, was 0.05, 0.1, 0.25, 0.5, or 1.0 in the different hydrogels. Then the mixtures were homogenized again at the same conditions. Each sample was loaded into an airtight syringe, which was kept at 40 °C for 1 h, transferred to a glass Petri dish (50 mm in diameter), and left to react for 24 h at room temperature. The formed hydrogels were removed, washed in cold water (8 °C) until they attained a pH of 6.5, and freeze-dried. Control hydrogels were prepared at identical R values and processing protocols as the MIHs but without adding *o*-xylene.

Structural Analysis of MIH$_{o\text{-Xylene}}$ by Fourier Transform Infrared Spectroscopy. Lyophilized MIH$_{o\text{-xylene}}$ ($R = 0.25$) and its control were ground and mixed with dry KBr (ratio 1:100). Pellets were formed with the aid of a mechanical press at 10 tons of pressure. Spectra were recorded on a Bruker IFS-66v (Bruker, Ettlingen, Germany) instrument in transmission mode. A total of 32 scans were collected with a resolution of 4 cm^{-1}.

Template Extraction. Approximately 50 mg of lyophilized MIH$_{o\text{-xylene}}$ and their corresponding controls were added to 100 mL of 1 M acetic acid solution under mechanical stirring for 4 h, separated by filtering through filter paper, dried at room temperature, and ground into a fine powder. A 1 mL aliquot from each solution was taken at

time intervals of 30 min, 1, 2, 3, and 4 h, placed into a septum vial, and kept at 40 °C for 30 min. Subsequently 50 μL from the headspace volume was injected into a gas chromatograph coupled to a mass spectrometer (GC-MS) to detect the *o*-xylene in the solution. A sample of the *o*-xylene standard was also injected from the headspace volume. The equipment used was a GC Varian 3400 coupled to a MS Saturn 3. The column was a F4 VF-5 capillary column (Varian, Inc., 30 m × 0.25 mm i.d. and 0.25 μm in thickness), and the oven temperature program was: started at 40 °C for 1 min, raised to 75 °C at 50 °C/min, raised further to 115 °C at 94 °C/min, and kept at this temperature for 2 min. The pressure of the carrier gas (helium) was set to 12 psi. The temperature of the injector was was 120 °C (splitless for 45 s), and the transfer line was also operated at 120 °C. The MS detector worked at 70 eV in ion trap mode; the final trap temperature was 200 °C. The scan was made from 45 to 600 *m*/*z* (6 scan s^{-1}). Xylene isomers of M^+ 106 and 91 *m*/*z* were monitored.

Scanning Electron Microscopy. The surface morphologies of dry hydrogels of CS−GNP and CS−GNP−*o*-xylene before and after acidic aqueous extraction were determined using scanning electron microscopy (JEOL, JSM 6400). Hydrogels were mounted on a brass mount and sputtered with Au−Pd in a Balzers SCD 004 sputter coater.

Adsorption of *o*-Xylene on $MIHs_{o\text{-Xylene}}$. Three milligrams of each $MIH_{o\text{-xylene}}$ and its controls prepared at different *R* values were placed in Eppendorf vials to which 1.5 mL of a 1000 ppm *o*-xylene diluted aqueous solution were added. The tubes were shaken vigorously and left to stand for 24 h at room temperature; afterward the solutions were filtered, and a 1 mL aliquot was used for *o*-xylene chromatographic analysis as described above. The concentration of *o*-xylene adsorbed by the tested materials was calculated by a comparison of the chromatographic peak areas with a peak of a 1000 ppm *o*-xylene standard solution.

Binding Affinity Studies. *o*-Xylene aqueous diluted solutions were prepared at 1000, 900, 500, 200, 100, 10, and 1 ppm. Three milligrams of $MIH_{o\text{-xylene}}$ at $R = 0.25$ or its control were placed each into an Eppendorf vial to which 1.5 mL of each of the different *o*-xylene solutions were added. The tubes were shaken vigorously and remained standing for 24 h at room temperature; afterward the solutions were filtered, and an aliquot of 1 mL was used for GC-MS analysis as described above. For each test, a standard *o*-xylene solution of the corresponding concentration was also injected. The adsorbance assumed to be in equilibrium, Q_e, was calculated based on the difference of *o*-xylene concentration between the standard solution and the test solution after adsorption at each concentration, the volume of aqueous solution, and the weight of the $MIH_{o\text{-xylene}}$, according to

$$Q_e = (C_o - C_e)V/W \quad (1)$$

where C_o is the initial *o*-xylene concentration (mg/mL), C_e is the *o*-xylene concentration (mg/mL) after 24 h, *V* is the volume of *o*-xylene solution (mL), and *W* is the weight of the $MIH_{o\text{-xylene}}$ (g). Adsorption was reported as the percentage of *o*-xylene bound by the $MIH_{o\text{-xylene.}}$

MIH Selectivity. *o*-Xylene, *m*-xylene, *p*-xylene, and 2-fluorotoluene aqueous diluted solutions were prepared at 1000 ppm. Three milligrams of $MIH_{o\text{-xylene}}$ at $R = 0.25$ or its control were placed each into an Eppendorf vial to which 1.5 mL of each of the different xylene or 2-fluorotoluene solutions were added. The filtrate was used for GC-MS analysis as described for the procedure for the adsorption tests above. A standard solution for each compound was injected, and all determinations were conducted in triplicate.

Results and Discussion

General Properties of CS−GNP Hydrogels. Before attempting to prepare CS−GNP molecularly imprinted hydrogels, the kinetics of gel formation and rheological properties of the CS−GNP system were studied as a function of cross-linking degree, *R*, to establish suitable conditions to prepare the MIHs. In general, the gelation time of the various CS−GNP mixtures at 40 °C was approximately ~2 h. At the early stages of the reaction, the CS−GNP mixture was colorless, clear, and viscous, while with time it gradually turned slightly yellow or green-yellow and eventually adopted a blue coloration concomitant with the setting of a gel. As *R* decreased, the formed gels were mechanically weaker and developed a pale blue color. While at greater *R* values, the formed gels were stiff and brittle and developed a deep blue color that showed a gradient from the surface in contact with air to the bottom.

Blue color formation in CS−GNP gels has been well-documented and attributed to the reaction between genipin and oxygen from air.[36,38] The formation of blue pigments in these systems has been ascribed to the oxygen-radical-induced polymerization of GNP and dehydrogenation of an intermediate compound that could only occur once the first series of cross-linking reactions had taken place.[38] In turn, chemical cross-linking in CS−GNP gels in acidic media has been suggested to take place through two distinct reactions.[38] The first and faster reaction is a nucleophilic attack on the genipin C3 carbon atom by a primary amine group causing the opening of the dihydropyran ring of GNP and resulting in the formation of a heterocyclic compound of GNP linked to the glucosamine residue in chitosan. The second and slower one is the nucleophilic substitution of the ester group of genipin (C11) to form a secondary amide linkage with chitosan. The genipin intermediate compounds could further associate to form cross-linked networks with short chains of cross-linking bridges. The proposed general cross-linking mechanism for this reaction is shown in Figure 1.

Evolution of G' and G'' Moduli during Gelation and Determination of the Critical Gel Time, t_{gel}. Continuous monitoring of the storage, $G'(t)$, and loss $G''(t)$ viscoelastic moduli and of the loss tangent, tan δ, by means of small-deformation dynamic rheology allowed the investigation of the evolution of the mechanical properties of CS−GNP hydrogels during the course of the cross-linking reaction. A representative result of the series of CS−GNP hydrogels of varying *R* values is shown in Figure 2. Inspection of the plot reveals that initially the system behaves like a viscous liquid ($G'' > G'$) and, gradually, $G'(t)$ starts to increase to the point where it crosses over and surpasses the $G''(t)$ trace, both traces describing a sigmoidal plot. These changes are accompanied by the pronounced decrease of the tan δ trace. The rheological behavior of the system with time has all of the typical hallmarks of a sol−gel transition process, occurring at a given critical time, subsequently referred here to as the critical gel time (t_{gel}). Theoretically, the critical gel point is identified with the instant of the onset of incipient formation of a gel network in the system or the percolation threshold (i.e., where the system is assumed to have formed the first cluster of infinite molecular mass).

Precise measurement of t_{gel} was of key importance to establish the best conditions to prepare $MIH_{o\text{-xylene}}$. Several methods based on the change of the mechanical properties have been proposed for determining t_{gel} for chemically and physically cross-linked gel network systems.[44,45] The criterion adopted in the present study to determine t_{gel} was given by the time elapsed up to the point of crossover of G' and G''.[46] Critical gel times calculated under this condition in polymer gels are known to be dependent on frequency, ω, and hence a different criterion, based on the determination of the crossover of tan δ traces registered at various ω values, has been proposed to circumvent this problem

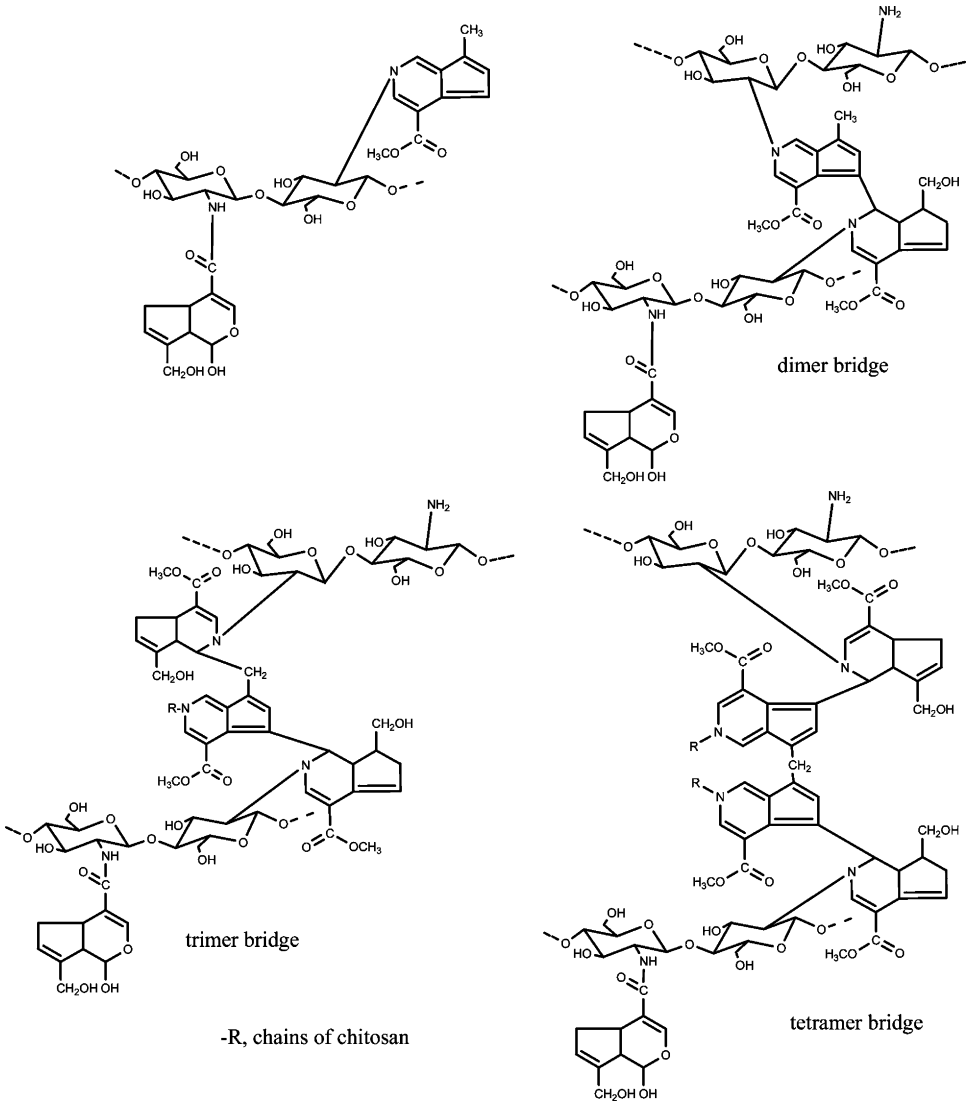

Figure 1. Schematic mechanism for chitosan cross-linking by genipin in acidic media proposed by Mi et al.[36]

by Winter and Chambon.[46] However, in many instances, the application of the Winter−Chambon criterion is experimentally not feasible, and rheological measurements at the critical gel point cannot be warranted at the linear viscoelastic region. Hence, in this work, t_{gel} was identified as the instant of the incipient prevalence of G' over G'' (i.e., when tan $\delta = G''/G'$ becomes just less than 1.00).[47] This pragmatic approach has been applied to determine critical gel point values in studies of other polysaccharide gel systems such as pectin−calcium[48] and hydrophobically modified chitosan[49] systems.

Influence of *R* on Gelation Kinetics and G'_{eq}. Figure 3a shows the variation of t_{gel} versus R for CS−GNP hydrogels at a constant CS concentration (1.5% (w/w)). Data were fitted to the model proposed by Ross−Murphy[44] using the nonlinear least-squares Levenberg−Marquardt iterative procedure available in OriginPro 7.5. In the model (see inset in Figure 3a) k is the rate constant, n' is the true reaction order of the process, p is an exponent with values $0 < p < 3$, and R_0 is the critical degree of cross-linking below which the system does not attain its percolation point. Restricting the values of the parameters as follows, $2.0 < n' < 4.0$, $R_0 \geq 0.008$, and $0.2 < p < 2$, best fit values of each were $n' = 3.02$, $k = 20758.21\ s^{-1}$, $R_0 = 0.01$, and $p = 0.26$. Critical gel time and G'_{eq} values obtained in CS−GNP gels in this study were similar to the ones found by Butler et al.[38] in the only other previous work of which we are aware addressing the rheological behavior of CS−GNP gels. Knowledge of the critical gelling conditions of the CS−GNP gels was central to the control of the system to design optimal conditions for the preparation of MIH matrixes.

Figure 3b shows the variation of the equilibrium storage moduli, G'_{eq}, values with R. In the same plot are also shown the values of the extent of cross-linking determined by the ninhydrin reaction. It can clearly be appreciated that both parameters hold very close agreement in their dependence on R. This can be ascribed to the formation of a more dense gel network as the stoichiometric amount of genipin increases up to a point ($R \approx 0.25$) beyond which it seems that there is no further formation of elastically active connections in the gel network. The extremely close agreement between the rheological results and those of the chemical determination of free amino groups by ninhydrin assay is consistent with this proposal. In a recently documented study on chitosan microsphere hydrogels cross-linked with genipin, it was also found that the extent of the cross-linking reaction proceeds up to a maximum limit.[33] The pattern of behavior observed in CS−GNP gel formation may stem from the cross-linking reaction mechanism between chitosan and genipin that entails the formation of di-, tri-, and tetramer cross-linking bridges[36] of the polymerized genipin units

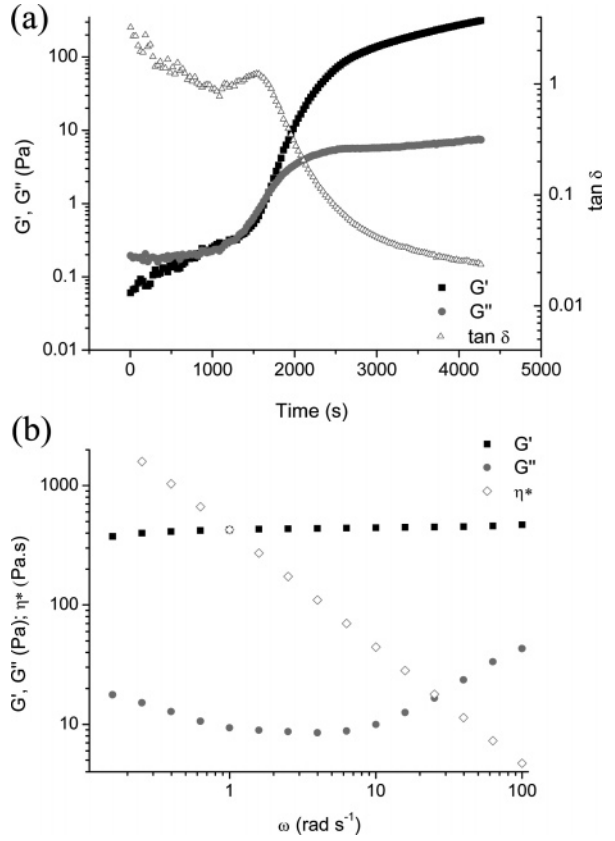

Figure 2. (a) Variation of the viscoelastic moduli, G' and G'' (ω = 1.0 rad s^{-1}, γ = 10%), of a CS−GNP hydrogel formed from a chitosan solution (1.5% (w/w) in 0.1 M acetic acid, R = 0.5, T = 40 °C). (b) Frequency dependence of G', G'', and the complex viscosity, η^* (γ = 10%), of the gel in part a after 1.5 h.

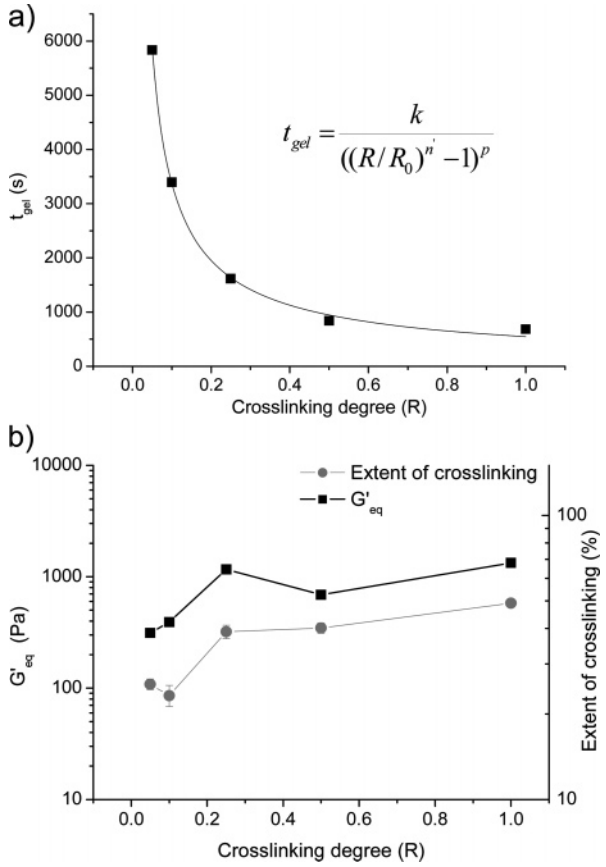

Figure 3. (a) Variation of t_{gel} (ω = 1 rad s^{-1}, γ = 10%, T = 40 °C) with R for CS−GNP gels at a constant chitosan concentration (1.5% (w/w) in 0.1 M acetic acid) and the nonlinear best fit of Ross-Murphy's model, (b) Dependence of G'_{eq} at 1.8t_{gel} (ω = 1 rad s^{-1}, γ = 10%, T = 40 °C) and extent of cross-linking on R for gels as in part a.

(Figure 1) and, hence, also on the very complex multiplicity and limited availability of the genipin monomer for cross-linking.

Yet another key aspect to investigate in the addressed CS−GNP hydrogels was the diffusion of water at varying R values. To this end, pulsed field gradient magnetic resonance techniques using strong field gradients (either in NMR or MRI) have proved, in previous studies, to be a very powerful tool in the study of slow diffusion processes in polysaccharide gels, including alginate,[50,51] dextran,[52] gellan,[53] and agarose.[54]

The MRI results registered for the CS−GNP system shown in Figure 4a reveal that in general the apparent diffusion coefficient, D, decreases as the degree of cross-linking increases. Although at very low degrees of cross-linking (R = 0.05−0.1) there is an abrupt decrease in D, this is followed by a nonlinear monotonic decreasing trend. It is interesting to observe that the pattern exhibited by D does not follow the expected reciprocal behavior of G'_{eq} nor that of the ninihydrin assay data (Figure 3b), particularly at high extents of cross-linking where one would expect little further variation in D. To account for this, we can argue that the molecular mobility of water does not seem to be governed only by the net cross-linking density of the gel network but perhaps also due to the entrapment of water in hydrophobic domains in the gel structure associated with the formation of the already mentioned genipin di-, tri-, and tetramer bridges. Figure 4b includes representative D coronal images of CS−GNP hydrogels showing the ROIs considered in the determinations.

Gelation of CS−GNP−*o*-Xylene. The first step of the experimental protocol used to prepare molecularly imprinted CS−GNP hydrogels with *o*-xylene involved vigorous mixing of *o*-xylene into the CS solution followed by addition of genipin methanolic solution, yielding a milky yellowish emulsion. Meanwhile, control CS−GNP solutions had a translucent yellow color. As gelation proceeded, a gradual color gradient was observed from the gel surface inward, going from deep blue to yellow. Once fully set, the hydrogels were thoroughly washed, lyophilized, and dried and invariably acquired a uniform deep blue color.

It was interesting to notice that when *o*-xylene was present in the CS−GNP system t_{gel} was delayed by ~18 min with respect to the control gel (Figure 5). Also in Figure 5 it was noticeable that at times prior to the onset of gel formation ($t < t_{gel}$) the CS−GNP−*o*-xylene solution mixture had lower G'' and G' values than the corresponding CS−GNP control hydrogel. This is attributed to the presence of small droplets of emulsified *o*-xylene in a solution of lower viscosity than the chitosan solution. The reduction of the volume fraction of chitosan and genipin in presence of *o*-xylene can also explain the longer t_{gel} value found in these gels with respect to the control ones. Also, G'_{eq} values revealed that CS−GNP−*o*-xylene hydrogels formed slightly weaker networks than those of CS−GNP control hydrogels, with values of 1526 and 1787 Pa, respectively. This difference was not of practical significance as both materials had a sufficiently firm structure so as to be handled perfectly during the preparation of the MIHs and control gels.

Structural Analysis of the CS−GNP−*o*-Xylene Complex. The formation of a complex between CS, GNP, and *o*-xylene was probed in the solid samples by transmission Fourier transform infrared (FTIR) spectroscopy. In Figure 6 are shown FTIR spectra recorded for KBr pellets of a CS−GNP control

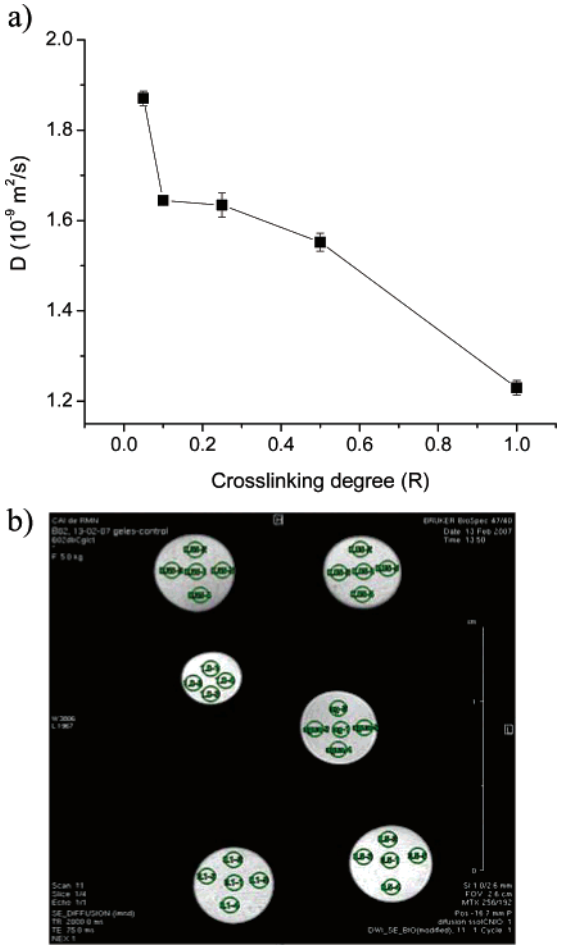

Figure 4. (a**)** Dependence of the apparent diffusion coefficient on the cross-linking degree of CS−GNP gels at a constant chitosan concentration (1.5% (w/w) in 0.1 M acetic acid) and (b) MRI coronal slice images of the same gels as in part a showing the ROIs used in the calculations of *D*.

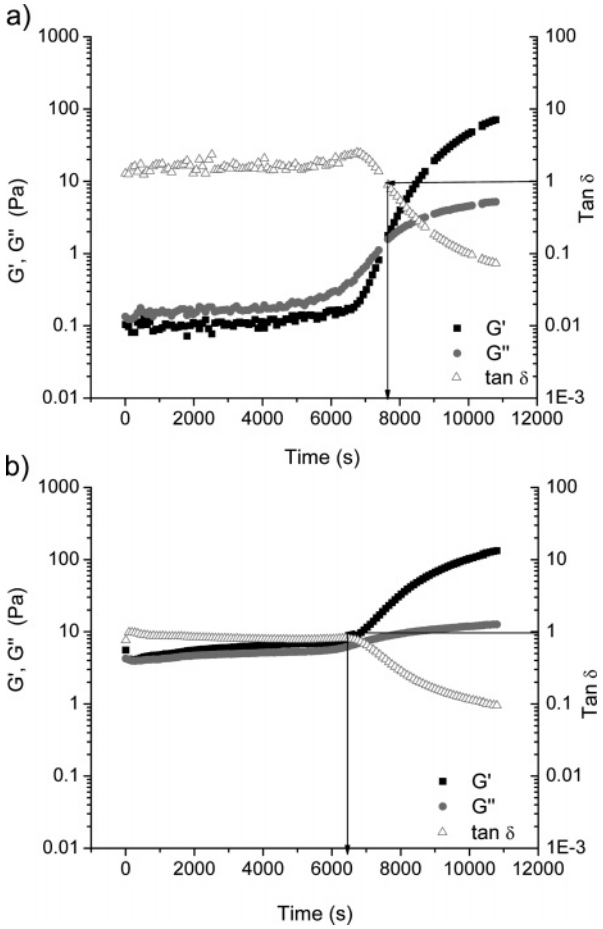

Figure 5. Variation of viscoelastic, *G*′ and *G*′ ($\gamma = 10\%$, $\omega = 1.0$ rad s^{-1}), moduli with time of (a**)** CS−GNP−*o*-xylene prepared with chitosan (1.5% (w/w) in 0.1 M acetic acid at 40 °C) cross-linked with genipin at $R = 0.05$ and *o*-xylene (*o*-xylene/glucosamine molar ratio = 10) and (b**)** a control gel prepared in the same conditions as in part a but without adding *o*-xylene.

(Figure 6a), CS−GNP−*o*-xylene complex (Figure 6b), and MIH$_{o\text{-xylene}}$ (Figure 6c) obtained for dried hydrogels prepared at $R = 0.25$ and a *o*-xylene/glucosamine molar ratio of 10. Close inspection of the figure reveals that there are only subtle differences between the three spectra in the bands indicated by the dashed lines. In particular, the band centered at 743 cm^{-1} (δ_{oop} and γ characteristic of ortho-di-substitution on benzene derivatives) can be singled out in the spectra of the CS−GNP−*o*-xylene analyte complex (Figure 6b). Also, the band located at ∼874 cm^{-1} appears split into two sharp bands in this same spectrum while appearing as a single band in the spectra of the CS−GNP control (Figure 6a) and MIH$_{o\text{-xylene}}$ (Figure 6c). A third difference was found in the width of the large band whose maximal intensity is centered at ∼3430 cm^{-1}, characteristic of ν(O−H) vibration, because in the spectrum of the CS−GNP−*o*-xylene complex it appears somewhat sharper by ∼350 cm^{-1} than in the other two spectra. In the same interval spanned by the ν(O−H) band it can also be appreciated that the signal centered at ∼2930 cm^{-1} (assigned to ν(N−H)) also appeared sharper in the spectrum of the CS−GNP−*o*-xylene complex than in those of the control and MIH$_{o\text{-xylene}}$. Altogether, these differences can be considered as providing evidence that the CS−GNP−*o*-xylene hydrogel retained *o*-xylene within its structure, possibly via cooperative weak noncovalent interactions such as $\pi-\pi$, van der Waals, and hydrophobic forces.[55] These interactions seem to perturb the hydrogen bonding involving −OH and −NH groups in the CS−GNP−*o*-xylene hydrogel, as demonstrated by the reduction in the width of the band centered at ∼2930 cm^{-1} of ν(O−H). The width of this band is well-known to be affected by hydrogen bonding in polysaccharides. In this respect, it is worth stressing that it is the specific steric arrangement adopted by the gel network when it interacts with the template that ultimately determines the subsequent recognition capacity of the MIH toward the analyte. In principle, steric memory in the MIH network is the result of the creation of specific arrangements in the covalently linked network of the CS−GNP−*o*-xylene complex as it binds the template and attains its lowest-energy state.

Once retention of *o*-xylene in the CS−GNP−*o*-xylene complex was proven, the template was extracted in acidic media to release *o*-xylene from the binding sites and make them available for further selective rebinding. The FTIR spectra of the solid material after extraction of *o*-xylene is shown in Figure 6c. Close inspection of this spectrum reveals the absence of the characteristic bands of the *o*-xylene at 743 cm^{-1}, which highlights the success of the extraction process. In addition to the FTIR spectroscopic evidence, we also analyzed the concentration of *o*-xylene at different time intervals in the aqueous extraction solution by GC-MS, and it was also confirmed that after 4 h of extraction no *o*-xylene peak was found in the chromatograms of any of the imprinted gels at varying *R* values (Supporting Information).

To obtain further understanding of the microstructure of the developed materials scanning electron microscopy was used.

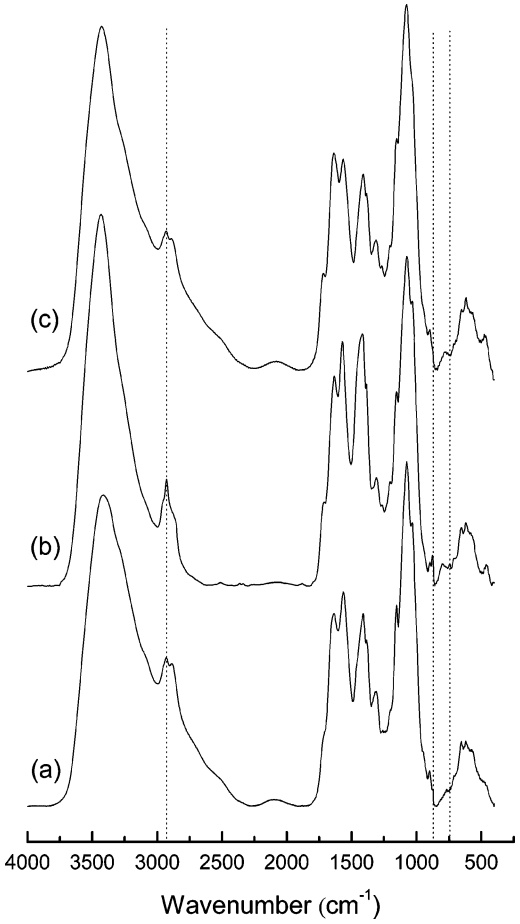

Figure 6. FTIR spectra (in KBr pellets) of CS−GNP dried powders made from: (a) CS−GNP hydrogel (1.5% (w/w) chitosan in 0.1 M acetic acid, $R = 0.25$); (b) CS−GNP−*o*-xylene template complex hydrogel; and (c) similar material as in part b after template extraction in 1 M acetic acid ($MIH_{o\text{-xylene}}$).

Figures 7a and 7b show micrographs of lyophilized CS−GNP and CS−GNP−*o*-xylene complexes, respectively, at $R = 0.25$ before the acidic aqueous extraction, while Figures 7c and 7d show the corresponding micrographs of the materials after the extraction. It was very interesting to notice that the CS−GNP−*o*-xylene complex (Figure 7b) revealed the presence of globular structures at the surface of the solid network. These structures are absent in both the control and the extracted materials. This gives physical evidence of the presence of *o*-xylene within the gel structure that remained trapped as emulsified droplets even after the freeze-drying process. This result is consistent with those obtained by FTIR and GC-MS that show that the *o*-xylene is retained in the CS−GNP−*o*-xylene complex and thereafter fully removed by the extraction process.

Photographs of the macroscopic appearance of the materials shown in the scanning electron micrographs are included in Figure 8. It can be appreciated that the final materials were easily made into a fine dry powder, an advantage for the development of materials for various applications (e.g., chromatographic supports, adsorbent materials, filter beds, etc.).

Adsorption Experiments. Once the general protocol for CS−GNP−*o*-xylene hydrogel preparation and template extraction was set up, molecularly imprinted and control hydrogels at varying *R* values were prepared to find the optimal cross-linking degree that would allow for greater *o*-xylene adsorption. It is known that an increase in cross-linking density makes chains more rigid, and this leads to an improvement in the stability of the system and to the creation of binding sites.[21] It was therefore of great interest to study the adsorption capacity of $MIH_{o\text{-xylene}}$ prepared at varying cross-linking degrees. To this end, the relative amount of *o*-xylene adsorbed by $MIH_{o\text{-xylene}}$ of varying *R* values from an aqueous solution was measured. The results in Figure 9 show that there were not major differences in the *o*-xylene adsorption versus the corresponding CS−GNP control gels, except for the $MIH_{o\text{-xylene}}$ at $R = 0.25$, which adsorbed 33% of the template while its control adsorbed only 15%. This difference can be attributable to the conformational memory created in the gel during the complex formation, when specific binding sites toward *o*-xylene were generated at an optimal *R* value. At *R* values below such optimal value, the diffusivity of *o*-xylene is expected to be high, because fewer cross-links in the gel network will result in larger pore sizes. In contrast, at high *R* values, the pore sizes decrease, and hence the diffusivity of *o*-xylene is bound to be restricted. This is consistent with previous studies in chitosan hydrogels cross-linked with glutaraldehyde and loaded with centchroman, where the drug loading was maximized at an optimal degree of cross-linking.[56]

When the cross-linking degree increased beyond $R = 0.25$, no further increase in the template adsorption was observed. This could be a consequence of the restriction to bulk water mobility (hence, also to *o*-xylene) and to diffusion imposed by the high degrees of cross-linking, as was confirmed by the apparent diffusion coefficient values (Figure 4).

However, notice that CS−GNP hydrogels (control gels) presented an inherent affinity toward *o*-xylene even though they had not been molecularly imprinted. This is probably due to hydrophobic interactions established between *o*-xylene and the macromolecular network. However, the quantity of *o*-xylene adsorbed by the control gels was in the range of 15−23%, which suggests that the adsorption in these gels is just a sorption process that has little to do with the existence of specific binding sites, as those present in $MIH_{o\text{-xylene}}$, particularly at $R = 0.25$, where the highest adsorption was observed. All further experiments with $MIH_{o\text{-xylene}}$ were thus prepared at $R = 0.25$.

In previous work conducted by Aburto and Le Borgne,[39] molecularly imprinted hydrogels of chitosan cross-linked with glutaraldehyde were prepared toward DBTS; they found that also there was a cross-linking degree that presented the highest template adsorption and beyond it the adsorption decreased.

MIH Capacity. The binding performance of the $MIH_{o\text{-xylene}}$ was characterized from the Langmuir and Freundlich adsorption isotherms, according to the equations given in the insets of Figures 10a and 10b, respectively. From the slope and intercept of the Langmuir isotherm, the values of *b* and Q_{max} were calculated to be 3.43 g/mL and 136.15 mg/g, respectively. While from the slope and intercept of the Freundlich linearized equation (Figure 10b), the *n* and Q_f values were 2.55 and 103.63 mg/g, respectively. Q_{max} and Q_f are directly related to the adsorption capacity of the $MIH_{o\text{-xylene}}$, while *b* is the adsorption equilibrium constant and 1/*n* represents the adsorption intensity. The adsorption capacity parameters of our MIH system were of the same order of magnitude as those recently published for molecularly imprinted chitosan beads toward hemoglobin.[41] It is worth mentioning that, in general, the range of documented values for the adsorption parameters obtained from Langmuir, Freundlich, and Scatchard treatments on MIPs is as wide as the number of different polymer matrix and template molecules used in their fabrication. Hilt and Byrne[13] have published a comparative list of adsorption parameters for a large number of MIP systems.

The fact that the linear correlation coefficient of the Freundlich equation ($R = 0.962$) was greater than that of the Langmuir

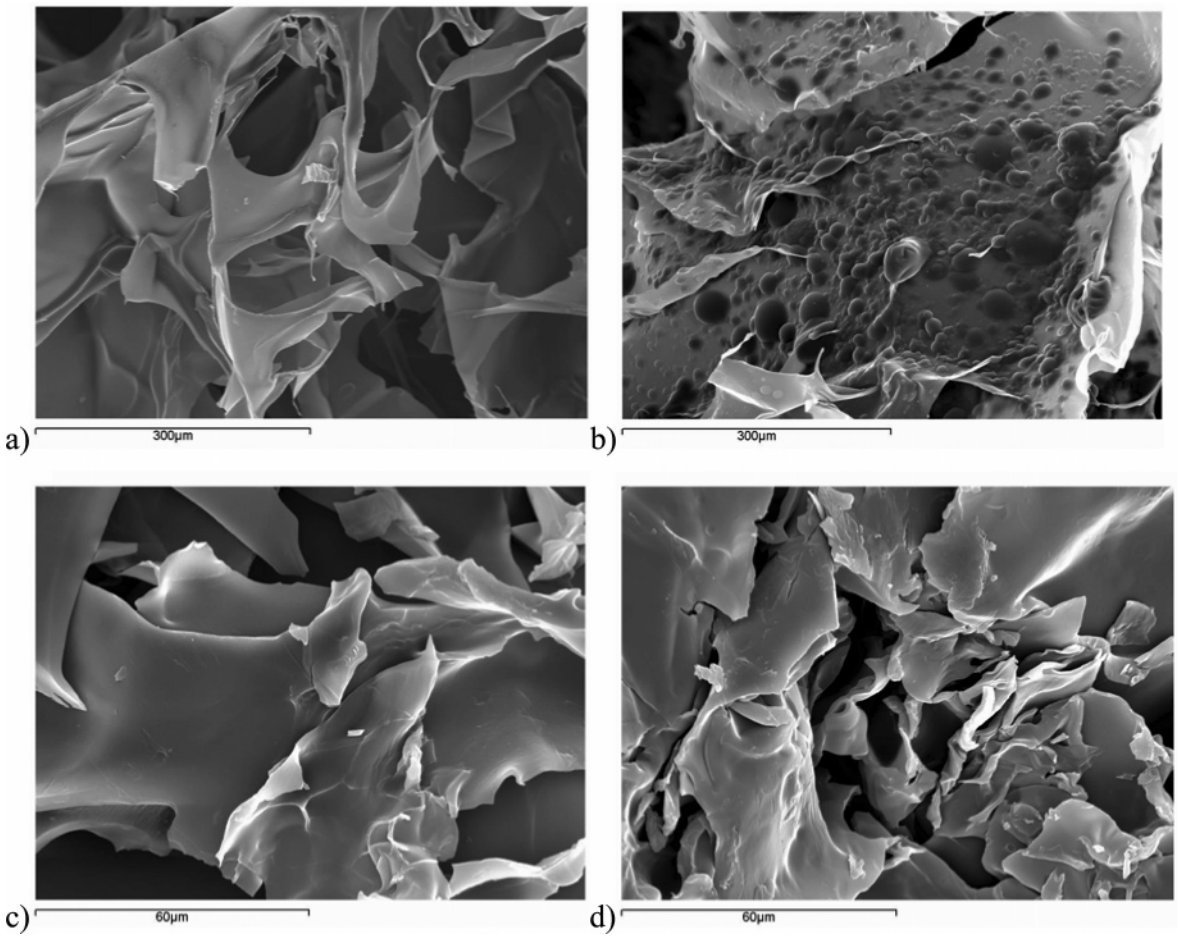

Figure 7. Scanning electron micrographs of dry CS−GNP hydrogels at $R = 0.25$: **(**a**)** control CS−GNP hydrogel; (b**)** CS−GNP−*o*-xylene complex before extraction; (c and d**)** corresponding micrographs for the same materials as in parts a and b, respectively, after acidic aqueous extraction. (Magnification is as given in the scale bars.)

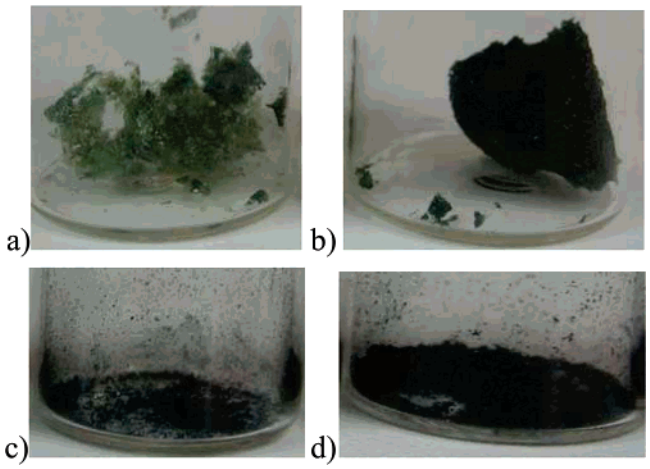

Figure 8. Photographs of the dry CS−GNP hydrogels at $R = 0.25$: (a**)** control CS−GNP hydrogel; (b**)** CS−GNP−*o*-xylene complex before extraction; **(**c and d**)** corresponding micrographs for the same materials as in parts a and b, respectively, after acidic aqueous extraction.

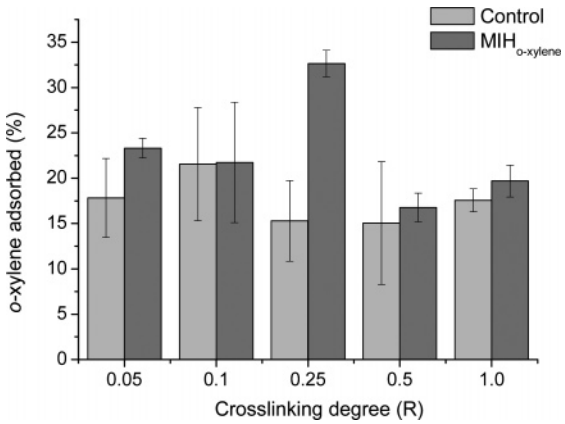

Figure 9. Variation of the relative adsorption of *o*-xylene from aqueous solution (1000 ppm *o*-xylene) by CS−GNP $MIH_{o\text{-xylene}}$ and their corresponding controls with cross-linking degree, *R*.

one ($R = 0.944$) is consistent with the notion that adsorption by $MIH_{o\text{-xylene}}$ is controlled predominantly by heterogeneous surface energy. This is in keeping with the well-documented pattern of behavior of molecularly imprinted polymers in which high and low affinity binding sites are commonly present.[13] It is likely that heterogeneous binding sites are thus created in the $MIH_{o\text{-xylene}}$, the expected consequence of the complexity of the cross-linking reaction between CS and GNP where di-, tri-, and tetrameric bridges are known to be formed.[36]

MIH Selectivity. To test in deeper detail the molecular imprinting effect, the selectivity of the $MIH_{o\text{-xylene}}$ was evaluated as the percentage of other *o*-xylene isomers adsorbed by the $MIH_{o\text{-xylene}}$ at $R = 0.25$ as compared to its control gel. Results included in Table 1 show that the highest adsorption was found for the $MIH_{o\text{-xylene}}$ (53.37%) when the template molecule itself was used in the rebinding experiment, while for *m*- and *p*-xylene the adsorptions were somewhat lower, 44.88% and 38.64%, respectively. Control CS−GNP hydrogels showed invariably

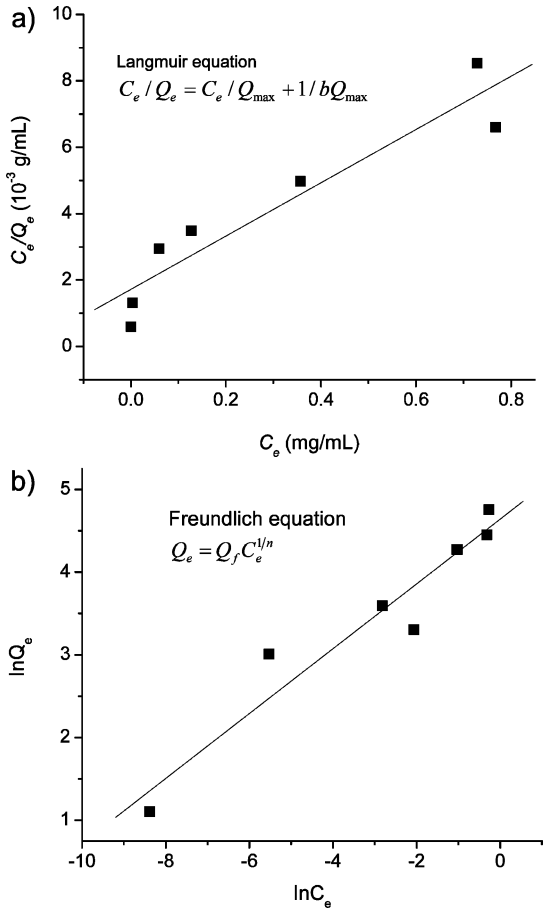

Figure 10. Adsorption isotherms of *o*-xylene on $MIH_{o\text{-xylene}}$ linearized according to **(a)** Langmuir and (b**)** Freundlich equations: $V = 1.5$ mL, $C = 1-1000$ ppm, sample weight = 3 mg, $T = 25$ °C, adsorption time = 24 h.

Table 1. Adsorption of PCB Analogue Molecules by a $MIH_{o\text{-xylene}}$ and Its Control Gel

	adsorbed quantity (%)	
molecule	control gel	$MIH_{o\text{-xylene}}$
o-xylene	20.50	53.37
m-xylene	16.71	44.88
p-xylene	30.04	38.64
2-fluorotoluene	47.16	10.88

lower adsorption capacities toward the three xylene isomers than $MIH_{o\text{-xylene}}$. In contrast, when a chemically different ortho-substituted aromatic compound was tested in rebinding experiments, namely, 2-fluorotuolene, the adsorption exhibited by $MIH_{o\text{-xylene}}$ decreased to 10.8%, though the control hydrogel unexpectedly showed high adsorption of this compound.

The selectivity displayed by $MIH_{o\text{-xylene}}$ could be explained on the basis of the electronic and steric properties of the template molecules and the binding sites in the molecularly imprinted network. The evidence is consistent with the idea that the steric effect played a key role in the recognition experiments. In this regard, during the formation of the CS−GNP−*o*-xylene complex between the hydrogel network and the template, "cavities" with steric memory toward benzene derivatives with a methyl substituent were created; hence $MIH_{o\text{-xylene}}$ was able to recognize the four tested molecules, as all of them share in common the presence of a methyl group in their structure. In addition to such steric effects, the low adsorption observed for 2-fluorotoluene is consistent with the notion that the creation of binding sites in $MIH_{o\text{-xylene}}$ was influenced not only by steric effects but also by the inherent electronic properties of the molecular species involved. The high electronegativity of the fluorine atom confers a permanent dipole moment (μ) to 2-fluorotoluene where the charge density is directed toward fluorine. In line with this argument, the dipole moment of 2-fluorotuolene, higher than that of any xylene isomer, could account for the lowest adsorption capacity observed in $MIH_{o\text{-xylene}}$ to this molecule. In addition, among xylene isomers, a decreasing trend was observed in the recognition capacity by $MIH_{o\text{-xylene}}$ concomitant with the decrease in dipolar moment too (*o*- > *m*- > *p*-xylene). Nevertheless, $MIH_{o\text{-xylene}}$ cannot distinguish unequivocally among specific xylene isomers. This is in contrast with other MIP materials that have proven to distinguish successfully even between chiral molecules.[57]

As already pointed out, the control gel also showed adsorption capacity for the xylene isomers tested and the for 2-fluorotoluene where the highest adsorption was observed. This affinity of CS−GNP for toward benzene derivatives can be attributed to noncovalent interactions between the template molecules and the cross-linked CS−GNP gel network, involving hydrophobic, Van der Waals, and $\pi-\pi$ electronic interactions. In the 2-fluorotoluene case, weak hydrogen bonds with fluorine may also account for the high adsorption by CS−GNP hydrogels. But in this case, the recognition phenomenon is not due to the formation of specific binding sites as in the $MIH_{o\text{-xylene}}$.

Hosoya et al. developed MIPs toward PCBs and dioxins utilizing xylene isomers as the template; they found that the positions of the substituents (*o*-, *p*-, and *m*-xylene) was very important to molecular recognition.[18,19] Their MIPs presented affinity toward xylene isomers, dichlorobenzenes, PCBs, and dioxins, but when dibromo-, dinitro-, or difluorobenzenes were used during recognition experiments, the adsorption decreased. They attributed those differences to the molecular shape and electronic properties of the molecules, but their results proved that xylene isomers could be used as analogue templates for molecular imprinting toward PCBs and dioxins.

Conclusions

The gelation process of chitosan with genipin is a slow reaction but allows for firm gels whose mechanical properties can be modulated by controlling the CS concentration and the degree of cross-linking. This study demonstrates that this hydrogel system is suitable to develop a molecularly imprinted material using xylene isomers as analogues of PCBs and dioxins. These results open the possibility of using this type of material for identification and/or separation purposes in various fields of application.

Acknowledgment. We are grateful to the Consejo Nacional de Ciencia y Tecnología (Mexico) for the financial support granted to this project (Grant No. 63450) and for a scholarship to B.M.E.G. and to Maria E. Fernández, B. Miralles, and G. Galed of the Instituto de Estudios Biofuncionales (IEB), Universidad Complutense de Madrid, Spain. Support from the Programa Iberoamericano de Ciencia y Tecnología para el Desarrollo (Spain) and the Sociedad Iberomericana de Quitina for the stay of B.M.E.G. at IEB is also gratefully acknowledged.

Supporting Information Available. GC-MS chromatograms of the acidic solution used to extract *o*-xylene from the CS−GNP−*o*-xylene complex. This material is available free of charge via the Internet at http://pubs.acs.org.

References and Notes

(1) Haupt, K. *Analyst* **2001**, *126*, 747.
(2) Haupt, K. *Anal. Chem.* **2003**, *9*, 376.

(3) Piletsky, S. A.; Alcock, S.; Turnen, A. P. F. *Trends Biotechnol.* **2001**, *19*, 9.
(4) Haupt, K.; Mosbach, K. *Trends Biotechnol.* **1998**, *16*, 468.
(5) Wulff, G.; Gross, T.; Schonfeld, R. *Angew. Chem., Int. Ed. Engl.* **1997**, *36*, 1962.
(6) Shea, K. J.; Sasaki, D. Y. *J. Am. Chem. Soc.* **1989**, *111*, 3442.
(7) Whitcomb, M. J.; Rodriguez, M. E.; Villar, P.; Vulfson, E. N. *J. Am. Chem. Soc.* **1995**, *117*, 7105.
(8) Mosbach, K.; Yu, Y.; Andersch, J.; Ye, L. *J. Am. Chem. Soc.* **2001**, *123*, 12420.
(9) Dhal, P. K.; Arnold, F. H. *J. Am. Chem. Soc.* **1991**, *113*, 7417.
(10) Dhal, P. K.; Arnold, F. H. *Macromolecules* **1992**, *25*, 7051.
(11) Krebs, J. F.; Borovik, A. S. *J. Am. Chem. Soc.* **1995**, *117*, 10593.
(12) Cormak, P. A. G.; Elorza, A. Z. *J. Chromatogr., B: Biomed. Sci. Appl.* **2004**, *804*, 173.
(13) Hilt, J. Z.; Byrne, M. E. *Adv. Drug Delivery Rev.* **2004**, *56*, 1599.
(14) Ikegami, T.; Lee, W. S.; Nariai, H.; Takeuchi, T. *Anal. Bioanal. Chem.* **2004**, *378*, 1898.
(15) Kubo, T.; Hosoya, K.; Watabe, Y.; Ikegami, T.; Tanaka, N.; Sano, T.; Kaya, K. *J. Chromatogr., A* **2004**, *1029*, 37.
(16) Matsui, J.; Fujiwara, K.; Takeuchi, T. *Anal. Chem.* **2000**, *72*, 1810.
(17) Matsui, J.; Fujiwara, K.; Ugata, S.; Takeuchi, T. *J. Chromatogr., A* **2000**, *889*, 25.
(18) Hosoya, K.; Yoshikako, K.; Sasaki, H.; Kimata, K.; Tanaka, N. *J. Chromatogr., A* **1998**, *828*, 91.
(19) Hosoya, K.; Watabe, Y.; Ikegami, T.; Tanaka, N.; Kubo, T.; Sano, T.; Kaya, K. *Biosens. Bioelectron.* **2004**, *20*, 1185.
(20) Lübke, M.; Whitcombe, M. J.; Vulfson, E. N. *J. Am. Chem. Soc.* **1998**, *120*, 13342.
(21) Byrne, M. E.; Park, K.; Peppas, N. A. *Adv. Drug Delivery Rev.* **2002**, *54*, 149.
(22) Peppas, N. A.; Huang, Y. *Pharm. Res.* **2002**, *19*, 578.
(23) Marx, S.; Zaltzsman, A. *Int. J. Environ. Anal. Chem.* **2003**, *83*, 671.
(24) Díaz-García, M. E.; Badía-Laíño, R. *Microchim. Acta* **2005**, *149*, 19.
(25) Berger, J.; Reist, M.; Mayer, J. M.; Felt, O.; Gurny, R. *Eur. J. Pharm. Biopharm.* **2004**, *57*, 19.
(26) Berger, J.; Reist, M.; Mayer, J. M.; Felt, O.; Gurny R. *Eur. J. Pharm. Biopharm.* **2004**, *57*, 35.
(27) Dambies, L.; Vincent, T.; Domard, A.; Guibal, E. *Biomacromolecules* **2001**, *2*, 1198.
(28) Shin, M. S.; Kim, S. J.; Park, S. J.; Lee, Y. H.; Kim, S. I. *J. Appl. Polym. Sci.* **2002**, *86*, 498.
(29) Gariepy, E. R.; Shive, M.; Bichara, A.; Berrada, M.; Garrec, D. L.; Chenite, A.; Leroux, J. C. *Eur. J. Pharm. Biopharm.* **2004**, *57*, 53.
(30) Borzacchiello, A.; Ambrosio, L.; Netti, P. A.; Nicolais, L.; Peniche, C.; Gallardo, A.; San Román, J. *J. Mater Sci.: Mater. Med.* **2002**, *12*, 861.
(31) Jin, J.; Song, M.; Hourston D. J. *Biomacromolecules* **2004**, *5*, 162.
(32) Chen, S.; Wu, Y. C.; Mi, F. L.; Lin, Y. H.; Yu, L. C.; Sung, H. W. *J. Controlled Release* **2004**, *96*, 285.
(33) Yuan, Y.; Chesnutt, B. M.; Utturkar, G.; Haggard, W. O.; Yang, Y.; Ong, J. L.; Bumgardner, J. D. *Carbohydr. Polym.* **2007**, *68*, 561.
(34) Sung, H. W.; Huang, R. N.; Huang, L. L.; Tsai, C. C. *J. Biomater. Sci., Polym. Ed.* **1999**, *10*, 63.
(35) Mi, F. L.; Tan, Y. C.; Liang, H. C.; Sung, H. W. *Biomaterials* **2002**, *23*, 181.
(36) Mi, F. L.; Sung, H. W.; Shyu, S. S. *J. Polym. Sci., Part A: Polym. Chem.* **2000**, *38*, 2804.
(37) Tsai, C. C.; Huang, R. N.; Sung, H. W.; Huang, C. L. *J. Biomed. Mater. Res.* **2000**, *52*, 58.
(38) Butler, M. F.; Yui-Fai, N.; Pudney P. D. A. *J. Polym Sci., Part A: Polym. Chem.* **2003**, *41*, 3941.
(39) Aburto, J.; Le Borgne, S. *Macromolecules* **2004**, *37*, 2938.
(40) Aburto, J.; Mendez-Orozco, A.; Le Borgne, S. *Chem. Eng. Process.* **2004**, *43*, 1587.
(41) Guo, T. Y.; Xia, Y. Q.; Hao, G. J.; Zhang, B. H.; Fu, G. Q.; Yuan, Z.; He, B. L.; Kennedy, J. F. *Carbohydr. Polym.* **2005**, *62*, 214.
(42) Xia, Y. Q.; Guo, T. Y.; Song, M. D.; Zhang, B. H.; Zhang, B. L. *Biomacromolecules* **2005**, *6*, 2601.
(43) Rinaudo, M.; Milas, M.; Le Dung, P. *Int. J. Biol. Macromol.* **1993**, *15*, 281.
(44) Ross-Murphy, S. B. *Rheol. Acta* **1991**, *30*, 401.
(45) Tung, C. Y. M.; Dynes, P. J. *J. Appl. Polym. Sci.* **1982**, *27*, 569.
(46) Winter, H. H.; Chambon, F. *J. Rheol.* **1986**, *30*, 367.
(47) Djabourov, M. *Polym. Int.* **1991**, *25*, 135.
(48) Durand, D.; Bertrand, C.; Clark, A. H.; Lips A. *Int. J. Biol. Macromol.* **1990**, *12*, 14.
(49) Félix, L.; Hernández, J.; Argüelles-Monal, W. M.; Goycoolea, F. M. *Biomacromolecules* **2005**, *6*, 2408.
(50) Simpson, N. E.; Grant, S. C.; Blackband, S. J.; Constantinidis I. *Biomaterials* **2003**, *24*, 4941.
(51) Potter, K.; Balcom, B. J.; Carpenter, T. A.; Hall, L. D. *Carbohydr. Res.* **1994**, *257*, 117.
(52) Watanabe, T.; Ohtsuka, A.; Murase, N.; Barth, P.; Gersonde, K. *Magn. Reson. Med.* **1996**, *35*, 697.
(53) Ohstsuka, A.; Watanabe, T. *Carbohydr. Polym.* **1996**, *30*, 135.
(54) Balcom, B. J.; Fischer, A. E.; Carpenter, A.; Hall, L. D. *J. Am. Chem. Soc.* **1993**, *115*, 3300.
(55) *Principles of Molecular Recognition*; Buckingham, A. D., Legon, A. C., Roberts, S. M., Eds.; Chapman & Hill: London, 1993.
(56) Gupta, K. C.; Jabrail, F. H. *Carbohydr. Polym.* **2006**, *66*, 43.
(57) Kondo, Y.; Yoshikawa, M. *Analyst* **2001**, *126*, 781.

BM700458A